LETTER

doi:10.1038/nature09570

Noise correlations improve response fidelity and stimulus encoding

Jon Cafaro[2] & Fred Rieke[1,2]

Computation in the nervous system often relies on the integration of signals from parallel circuits with different functional properties. Correlated noise in these inputs can, in principle, have diverse and dramatic effects on the reliability of the resulting computations[1–8]. Such theoretical predictions have rarely been tested experimentally because of a scarcity of preparations that permit measurement of both the covariation of a neuron's input signals and the effect on a cell's output of manipulating such covariation. Here we introduce a method to measure covariation of the excitatory and inhibitory inputs a cell receives. This method revealed strong correlated noise in the inputs to two types of retinal ganglion cell. Eliminating correlated noise without changing other input properties substantially decreased the accuracy with which a cell's spike outputs encoded light inputs. Thus, covariation of excitatory and inhibitory inputs can be a critical determinant of the reliability of neural coding and computation.

Differences in the properties of excitatory and inhibitory synaptic inputs to a target cell provide a key control of neural activity. Feedforward inhibitory synaptic input is a ubiquitous example. A delay in inhibitory input relative to excitatory input, for example by an extra synaptic delay in the circuit providing inhibitory input, can limit response duration to the time window in which the target cell receives excitatory but not inhibitory input[9]. More generally, inhibitory input can cancel unwanted responses by arriving before or at the same time as excitatory input[10–13]. Theoretical work illustrates how the effectiveness of these computations depends on the strength of covariation between excitatory and inhibitory synaptic inputs[8]. Thus, although synaptic noise will always decrease the reliability of the neural response, strong noise correlations, unlike independent noise, could allow fluctuations in inhibitory synaptic input to cancel corresponding fluctuations in excitatory synaptic input[5] (Fig. 1). Such noise correlations can arise if noise within excitatory and inhibitory pathways originates from a common source (Fig. 1, left), for example in densely and randomly connected recurrent networks[14]. Noise cancellation in synaptic integration could in turn reduce trial-to-trial variability in a cell's spike output (Fig. 1, right).

The extent and impact of noise correlations depends on several network and cellular properties, including nonlinearities in synaptic transmission[15] or spike generation[16] that could decrease correlation strength. This dependence makes it difficult to predict the importance of noise correlations from modelling alone or from correlations measured in cell pairs. Work on the retina provides a rare opportunity to provide quantitative experimental information about how noise correlations affect the coding of physiologically relevant stimuli. Our goal was first to measure covariation of the excitatory and inhibitory synaptic inputs received by a retinal ganglion cell (Fig. 1, (Q1)) and then to test how these noise correlations affect the encoding of light stimuli in a cell's spike output (Fig. 1, (Q2)).

Quantifying the covariation of excitatory and inhibitory synaptic input requires measuring these two conductances simultaneously or near simultaneously. To do this, we rapidly alternated the ganglion cell voltage between the reversal potentials for excitatory and inhibitory synaptic inputs, collecting a single sample of each input every 10 ms (Fig. 2a). Control experiments indicated that the voltage at the synaptic receptors had reached a near-constant value at these sampling times (Supplementary Fig. 1). This sampling rate is high in comparison with the 50–100 ms time course of a ganglion cell's response to light inputs. To check how well this procedure captured light-dependent changes in conductance, we compared the simultaneously measured conductances with those measured non-simultaneously when the voltage was held constant at the excitatory or inhibitory reversal potential. Mean excitatory and inhibitory conductances resulting from a repeated, modulated light input differed minimally (Fig. 2b). In 21 cells, the alternating voltage approach captured 99.9 ± 0.6% of the power of the conductance signal and 83 ± 4% of that of the conductance noise (mean ± s.e.m.; see Methods). Thus, simultaneous conductance measurements capture most of the structure in the synaptic inputs a ganglion cell receives.

Simultaneous conductances measured during constant light input often exhibited spontaneous excitatory synaptic events accompanied in time by inhibitory synaptic events (Fig. 2c, top, black arrowheads). Such events in fact typically occurred together. Correlated noise events were rarely observed during non-simultaneously measured conductances (Fig. 2c, bottom). Correspondingly, the cross-correlation function for

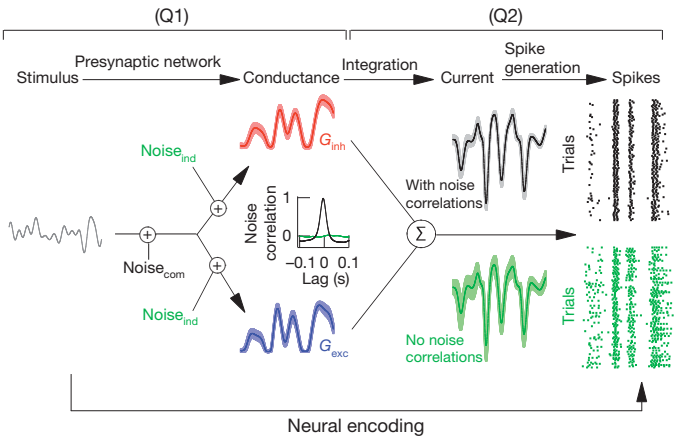

Figure 1 | Effects of noise correlations on the variability of synaptic current and spike output. Neural encoding consists of three basic steps: a stimulus shapes excitatory (blue, G_{exc}) and inhibitory (red, G_{inh}) synaptic conductances; these conductances then shape synaptic currents; and the resulting currents control spike generation to produce a sequence of action potentials (spikes). Noise correlations will be strong if a common source dominates noise in excitatory and inhibitory pathways ($Noise_{com}$) and minimal if the dominant noise source arises independently ($Noise_{ind}$). Correlated (black traces) as opposed to uncorrelated (green traces) noise between excitatory and inhibitory conductances can lead to lower variability of both the synaptic current and the spike output (shaded regions around traces). Understanding this issue requires answering two questions. (Q1) How much do converging excitatory and inhibitory input covary? (Q2) What is the impact of such noise correlations on the neural output?

[1]Howard Hughes Medical Institute. University of Washington, Seattle, Washington 98195, USA. [2]Department of Physiology and Biophysics, University of Washington, Seattle, Washington 98195, USA.

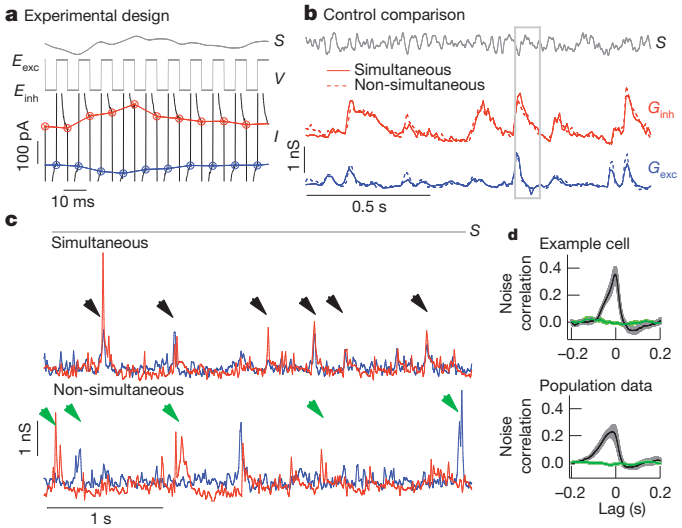

Figure 2 | Near-simultaneous recording of excitatory and inhibitory synaptic input to an ON–OFF directionally selective ganglion cell. **a**, Light stimulus (*S*) is presented while the voltage (*V*) of the cell alternates between the excitatory (E_{exc}) and inhibitory (E_{inh}) reversal potentials. Excitatory (blue) and inhibitory (red) synaptic currents (*I*) are sampled at the end of each voltage step. **b**, Conductances derived from measured currents (Methods) and averaged across multiple repeats of the same stimulus (*S*). Simultaneously measured conductances (solid lines) closely match those (dashed lines) measured non-simultaneously with the voltage held fixed at the reversal potentials for excitatory or inhibitory input (both excitatory and inhibitory correlations are 0.91 ± 0.01 (mean ± s.e.m.), 21 cells). **a** is an enlarged view of the boxed region of **b**. **c**, Top: section of simultaneously recorded conductances during constant light input shows correlated excitatory and inhibitory spontaneous events (black arrowheads). Bottom: non-simultaneously recorded conductances also show spontaneous events (green arrowheads), but they are rarely correlated. Records have been resampled at 50 Hz for comparison with the top conductances. **d**, Top: cross-correlation (mean ± s.e.m., 10 trials) of excitatory and inhibitory conductances in an example cell during simultaneous (black) and non-simultaneous (green) recording. Bottom, cross-correlation for all recorded cells (mean ± s.e.m., 6 cells).

simultaneously measured excitatory and inhibitory conductances during constant light input showed considerable structure, unlike the cross-correlation for non-simultaneously measured conductances (single cell: Fig. 2d, top; population: Fig. 2d, bottom). Thus, simultaneous conductance recordings revealed correlations between converging synaptic inputs that were inaccessible from more conventional recordings.

To determine both the strength of noise correlations during modulated light input and their effect on a cell's spike output, we first considered midget ganglion cells, which comprise the majority of ganglion cells in the primate retina[17]. Midget ganglion cells receive delayed feed-forward synaptic inhibition, where the delay reflects an extra synapse in the circuit controlling inhibitory input. Thus, excitatory input comes directly from bipolar cells, whereas inhibitory input comes from amacrine cells that themselves receive input from bipolar cells[18]. Similar delayed feed-forward inhibition is a characteristic of many cortical circuits, including hippocampus, cerebellum, barrel cortex and auditory cortex[9,11,12,19–21]. We simultaneously recorded excitatory and inhibitory synaptic inputs during a full-field modulated light stimulus (Fig. 3a, left) and estimated variability in the synaptic responses by subtracting the average synaptic input from each individual trial (Fig. 3a, right). The peak correlation strength of the resulting residuals ranged from 0.15 to 0.5 (Fig. 3b, black traces). Noise correlations in the interleaved non-simultaneous conductances were substantially smaller (Fig. 3b, green traces). Slow drift in the light response accounted for the remaining noise correlations in the non-simultaneous conductances (Supplementary Fig. 2).

The alternating-voltage technique could produce artefactual noise correlations by overshooting the appropriate reversal potentials for excitatory or inhibitory synaptic inputs. For example, holding at a voltage positive relative to the excitatory reversal potential could cause

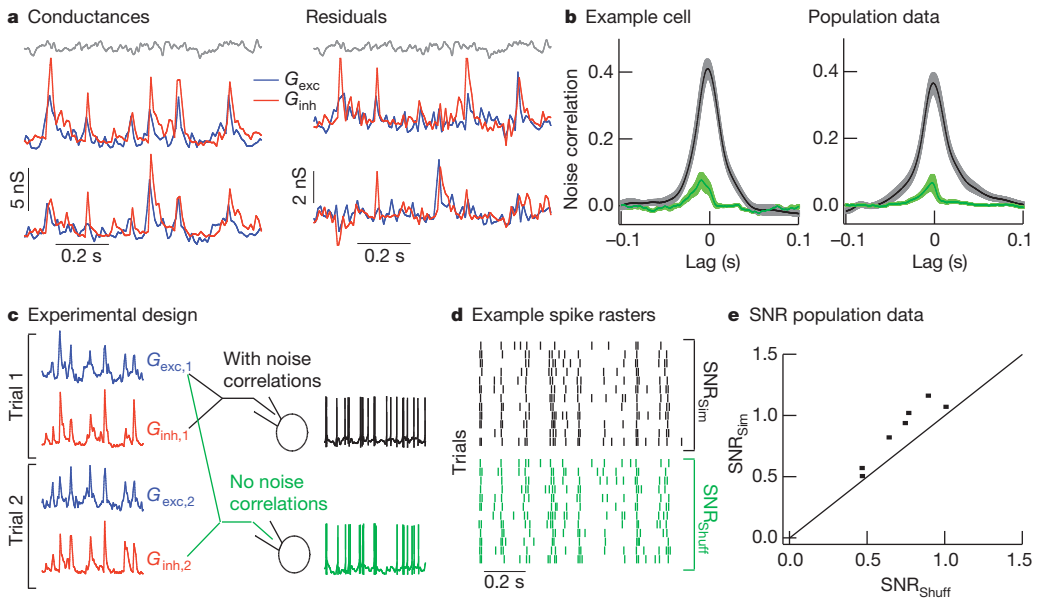

Figure 3 | Strength and impact of noise correlations in synaptic inputs to primate midget ganglion cells. **a**, Left: two trials of simultaneously recorded conductances during modulated light input (grey). Right: residual conductances (trials from left with mean subtracted), which estimate noise in each trial. **b**, Left: cross-correlation (mean ± s.e.m., 12 trials) of excitatory and inhibitory residual conductances in an example cell during simultaneous (black) and non-simultaneous (green) recording. Right: cross-correlation for all recorded cells (mean ± s.e.m., 15 cells). **c**, Logic of dynamic-clamp experiments using simultaneously or shuffled simultaneous conductances in place of synaptic input. **d**, Example spike trains from 12 dynamic-clamp trials of simultaneous conductances (black) or their shuffled counterparts (green). SNR, signal-to-noise ratio. **e**, Signal-to-noise ratio of spike trains generated from simultaneous conductances versus that of spike trains generated from shuffled conductances (dots). The signal-to-noise ratio for simultaneous conductances was 1.22 ± 0.04 times higher than that for shuffled conductances (mean ± s.e.m., 7 cells, $P = 0.0015$).

an increase in the excitatory conductance to be misinterpreted as an increase in both the excitatory and inhibitory conductances, thus leading to an artefactual correlation. A similar logic holds if a cell is held more negative than the reversal potential for inhibitory input. However, if anything the alternating-voltage technique fell short of the actual reversal potentials and hence underestimated the strength of noise correlations (Supplementary Fig. 3).

To determine the effect of covariation of excitatory and inhibitory synaptic inputs on a midget ganglion cell's response to physiological inputs, we compared the pattern of spikes produced by simultaneous (with noise correlations) and non-simultaneous (without noise correlations) conductances in dynamic-clamp experiments (Fig. 3c and Supplementary Fig. 4). The non-simultaneous conductances consisted of shuffled pairings of simultaneously recorded excitatory and inhibitory conductances; this procedure removed noise correlations while holding all other statistics constant. We compared the precision of the spike responses to the two sets of conductances by calculating the signal-to-noise ratio from repeated dynamic-clamp trials (Fig. 3d; see Methods). In all cases, the signal-to-noise ratio was higher for conductances with noise correlations (Fig. 3e). Quantifying the temporal precision of the spike responses using a spike distance metric[22,23] gave similar results (data not shown). Thus, the precision of a midget cell's output in response to light stimuli depends on the covariation of excitatory and inhibitory synaptic inputs.

Feed-forward synaptic inhibition can serve a more diverse functional role when the amplitude or timing of inhibitory input relative to excitatory input depends on the stimulus. For example, the ability of a subset of retinal ganglion cells to respond to the direction of a moving object[24,25] (Fig. 4a, b) relies on cancellation of excitatory input by inhibitory input in the non-preferred direction[10]. Covariation of excitatory and inhibitory synaptic inputs could make such a mechanism robust to noise, for example by preventing a larger-than-average excitatory synaptic event from overwhelming the corresponding inhibitory synaptic event and causing a response to movement in an inappropriate direction. To test this proposal, we recorded simultaneous conductances in mouse ON–OFF directionally selective ganglion cells (ON–OFF DSGCs) in response to a bar of light moving in different directions (Fig. 4a). Excitatory and inhibitory conductances showed strong noise correlations that were largely absent from non-simultaneous conductances (Fig. 4d; see Supplementary Fig. 5 for results from full-field light stimuli). Both excitatory and inhibitory conductances and the strength of the noise correlations depended on bar direction (Fig. 4c, d). For example, noise correlations in the non-preferred direction were three to four times stronger than those in the preferred direction. Furthermore, excitatory and inhibitory conductances showed near-perfect covariation in the non-preferred direction.

We tested the impact of noise correlations on direction tuning using simultaneous (with noise correlations) and non-simultaneous (without noise correlations) conductances in dynamic-clamp experiments; non-simultaneous conductances consisted of simultaneous conductances shuffled between trials but not bar directions. Both the mean and the standard deviation of the firing rate in the non-preferred direction were considerably higher for non-simultaneous conductances (Fig. 4e, f). The failure of a cell to attenuate its response reliably for movement in the non-preferred direction should negatively affect its ability to encode direction. Indeed, each recorded cell showed greater direction selectivity for the simultaneous conductances (Fig. 4g). Thus, the computation underlying directional selectivity depends on covariation of excitatory and inhibitory synaptic inputs and the resulting cancellation of noise shared between the circuits providing each type of input.

Computation in the retina follows a basic plan found in many other neural circuits: signals in a common population of inputs diverge to parallel and functionally dissimilar pathways, and integration of the signals from multiple parallel pathways governs the output of the circuit. Divergence into separate excitatory and inhibitory circuits is a prominent

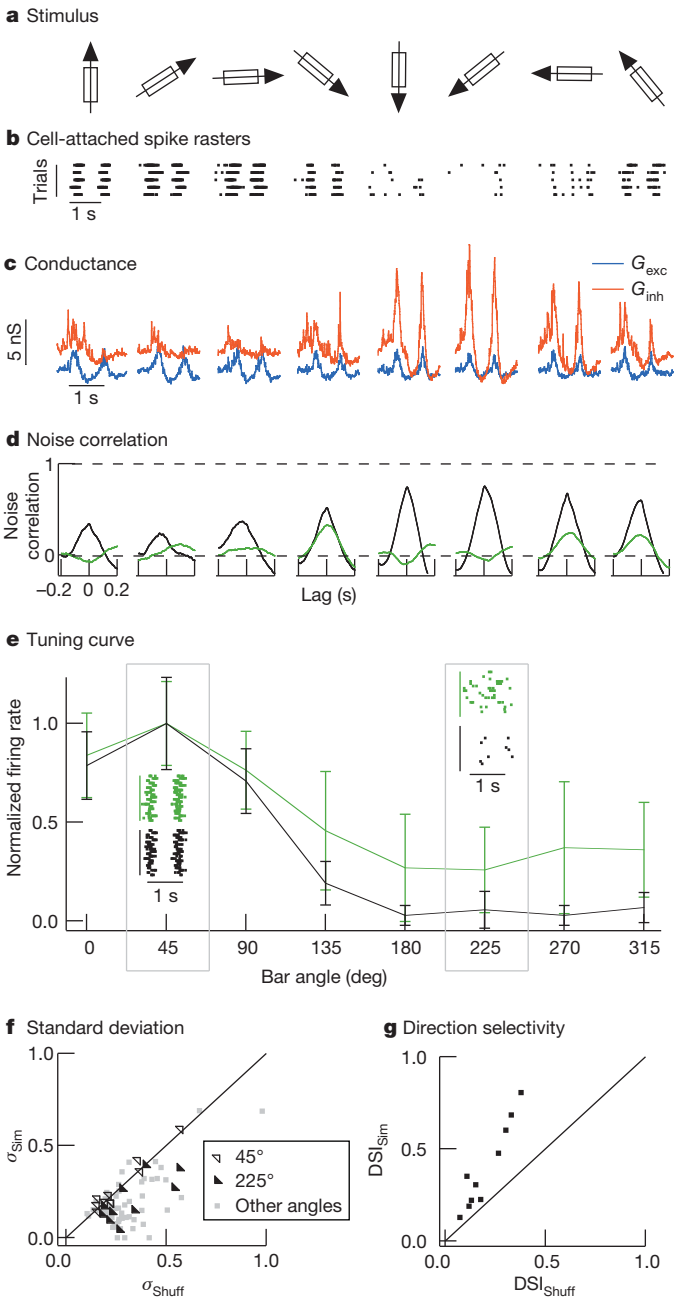

Figure 4 | Strength and impact of noise correlations in synaptic inputs to ON–OFF directionally selective ganglion cells. **a**, A bar of light was moved in eight directions, at 45° increments in random order. **b**, Extracellular (cell-attached configuration) spike responses to the moving bar. **c**, Examples of simultaneously recorded conductances showing tuning of excitatory (blue) and inhibitory (red) conductances. **d**, Simultaneous conductances (black) show strong noise correlations that are largely absent from the non-simultaneous conductances (green). **e**, Normalized directional tuning (spike count versus direction) from a single dynamic-clamp experiment (mean ± s.d.) for 20 trials of simultaneous or shuffled simultaneous conductances. Insets at 45° (preferred direction) and 225° (non-preferred direction) show spike rasters. **f**, Standard deviation of the normalized spike count is significantly smaller for simultaneous trials than for shuffled trials in non-preferred directions (135–315°; $P < 0.05$, 10 cells). Standard deviations in the preferred direction were similar. **g**, Direction selectivity index (DSI; see Methods) is 2.0 ± 0.2 times larger for simultaneous conductances than for shuffled conductances (mean ± s.e.m., 10 cells, $P = 0.0002$).

example of such a motif. Noise in shared inputs naturally causes covariation of signals in the parallel pathways. The strength of such noise correlations will depend on cellular properties within the network[15,16],

the stimulus delivered[26] (Fig. 4) and the state of the network[27]. Thus, excitatory and inhibitory inputs to cells in some, but not all, circuits are expected to show strong noise correlations, as indeed is the case in barrel cortex[27,28]. Here we put such noise correlations in the context of the coding of physiologically relevant stimuli. Our results reveal a critical role for noise correlations in maintaining appropriate cancellation of excitatory and inhibitory inputs and thus sharpening tuning to specific stimuli. This work provides an example of neurons that perform computations reliant on noise correlations. Given the prevalence of circuits in which feed-forward inhibition shapes neural responses[9,11,12,19–21], noise correlations probably have a similar role in other neural circuits.

METHODS SUMMARY

We took electrical recordings from midget ganglion cells in primate and ON–OFF DSGCs in mouse retinas using patch-clamp techniques as previously described[23,29]. Light stimuli were delivered from light-emitting diodes or an organic light-emitting diode monitor (eMagin). Mean light levels for all experiments were near 5,000 absorbed photons per cone per second.

The 10-ms cycle period during the simultaneous conductance recordings allows us to resolve input at 50 Hz and below. The fraction of the measured current variance at this cycle time was determined by calculating the fraction of the variance of the non-simultaneous (constant-voltage) conductances that can be accounted for by the variance of the simultaneous conductances.

Signal-to-noise ratios of spike outputs were calculated by forming spike trains of zeroes and ones from each trial, with 1-ms resolution. The mean and trial residuals of these spike trains were calculated and the power spectra of these functions were assessed and corrected for sample number bias[30]. Power spectra were integrated between 1 and 20 Hz and the result for the mean responses was divided by that for the residuals (Supplementary Fig. 6).

Spike number in ON–OFF DSGCs in response to the moving bar was summed over the entire duration of the bar's movement. The direction selectivity index[10] was calculated as $\mathrm{DSI} = |\sum \mathbf{v}_i / \sum \boldsymbol{r}_i|$, where $\mathbf{v}_i$ are vectors of lengths $\boldsymbol{r}_i$, equal to the normalized firing rate, and point in the direction of the moving bar that produced the presented conductances.

Current injected into a cell (I) during dynamic-clamp experiments[31] was calculated as

$$I(t) = G_{\mathrm{exc}}(t)(V(t-\Delta t) - E_{\mathrm{exc}}) + G_{\mathrm{inh}}(t)(V(t-\Delta t) - E_{\mathrm{inh}})$$

where G_{exc} and G_{inh} are a pair of conductances recorded during light stimulation, V is the cell's membrane potential, and E_{exc} and E_{inh} are reversal potentials set respectively at 0 mV and −80 mV. Changing the inhibitory reversal potential, E_{inh}, to −50 mV did not substantially affect the results.

Full Methods and any associated references are available in the online version of the paper at www.nature.com/nature.

Received 27 July; accepted 11 October 2010.
Published online 5 December 2010.

1. Shadlen, M. N. & Newsome, W. T. Noise, neural codes and cortical organization. *Curr. Opin. Neurobiol.* **4,** 569–579 (1994).
2. Softky, W. R. & Koch, C. The highly irregular firing of cortical cells is inconsistent with temporal integration of random EPSPs. *J. Neurosci.* **13,** 334–350 (1993).
3. Abbott, L. F. & Dayan, P. The effect of correlated variability on the accuracy of a population code. *Neural Comput.* **11,** 91–101 (1999).
4. Romo, R., Hernandez, A., Zainos, A. & Salinas, E. Correlated neuronal discharges that increase coding efficiency during perceptual discrimination. *Neuron* **38,** 649–657 (2003).
5. Salinas, E. & Sejnowski, T. J. Impact of correlated synaptic input on output firing rate and variability in simple neuronal models. *J. Neurosci.* **20,** 6193–6209 (2000).
6. Dan, Y., Alonso, J. M., Usrey, W. M. & Reid, R. C. Coding of visual information by precisely correlated spikes in the lateral geniculate nucleus. *Nature Neurosci.* **1,** 501–507 (1998).
7. Nirenberg, S., Carcieri, S. M., Jacobs, A. L. & Latham, P. E. Retinal ganglion cells act largely as independent encoders. *Nature* **411,** 698–701 (2001).
8. Averbeck, B. B., Latham, P. E. & Pouget, A. Neural correlations, population coding and computation. *Nature Rev. Neurosci.* **7,** 358–366 (2006).
9. Pouille, F. & Scanziani, M. Enforcement of temporal fidelity in pyramidal cells by somatic feed-forward inhibition. *Science* **293,** 1159–1163 (2001).
10. Taylor, W. R. & Vaney, D. I. Diverse synaptic mechanisms generate direction selectivity in the rabbit retina. *J. Neurosci.* **22,** 7712–7720 (2002).
11. Wilent, W. B. & Contreras, D. Dynamics of excitation and inhibition underlying stimulus selectivity in rat somatosensory cortex. *Nature Neurosci.* **8,** 1364–1370 (2005).
12. Wehr, M. & Zador, A. M. Balanced inhibition underlies tuning and sharpens spike timing in auditory cortex. *Nature* **426,** 442–446 (2003).
13. Leary, C. J., Edwards, C. J. & Rose, G. J. Midbrain auditory neurons integrate excitation and inhibition to generate duration selectivity: an *in vivo* whole-cell patch study in anurans. *J. Neurosci.* **28,** 5481–5493 (2008).
14. Renart, A. *et al.* The asynchronous state in cortical circuits. *Science* **327,** 587–590 (2010).
15. Trong, P. K. & Rieke, F. Origin of correlated activity between parasol retinal ganglion cells. *Nature Neurosci.* **11,** 1343–1351 (2008).
16. de la Rocha, J., Doiron, B., Shea-Brown, E., Josic, K. & Reyes, A. Correlation between neural spike trains increases with firing rate. *Nature* **448,** 802–806 (2007).
17. Dacey, D. M. & Petersen, M. R. Dendritic field size and morphology of midget and parasol ganglion cells of the human retina. *Proc. Natl Acad. Sci. USA* **89,** 9666–9670 (1992).
18. Calkins, D. J. & Sterling, P. Absence of spectrally specific lateral inputs to midget ganglion cells in primate retina. *Nature* **381,** 613–615 (1996).
19. Gabernet, L., Jadhav, S. P., Feldman, D. E., Carandini, M. & Scanziani, M. Somatosensory integration controlled by dynamic thalamocortical feed-forward inhibition. *Neuron* **48,** 315–327 (2005).
20. Luna, V. M. & Schoppa, N. E. GABAergic circuits control input-spike coupling in the piriform cortex. *J. Neurosci.* **28,** 8851–8859 (2008).
21. Mittmann, W., Koch, U. & Hausser, M. Feed-forward inhibition shapes the spike output of cerebellar Purkinje cells. *J. Physiol. (Lond.)* **563,** 369–378 (2005).
22. Victor, J. D. & Purpura, K. P. Nature and precision of temporal coding in visual cortex: a metric-space analysis. *J. Neurophysiol.* **76,** 1310–1326 (1996).
23. Murphy, G. J. & Rieke, F. Network variability limits stimulus-evoked spike timing precision in retinal ganglion cells. *Neuron* **52,** 511–524 (2006).
24. Barlow, H. B., Hill, R. M. & Levivk, W. R. Retinal ganglion cells responding selectively to direction and speed of image motion in the rabbit. *J. Physiol. (Lond.)* **173,** 377–407 (1964).
25. Weng, S., Sun, W. & He, S. Identification of ON-OFF direction-selective ganglion cells in the mouse retina. *J. Physiol. (Lond.)* **562,** 915–923 (2005).
26. Cohen, M. R. & Newsome, W. T. Context-dependent changes in functional circuitry in visual area MT. *Neuron* **60,** 162–173 (2008).
27. Gentet, L. J., Avermann, M., Matyas, F., Staiger, J. F. & Petersen, C. C. Membrane potential dynamics of GABAergic neurons in the barrel cortex of behaving mice. *Neuron* **65,** 422–435 (2010).
28. Okun, M. & Lampl, I. Instantaneous correlation of excitation and inhibition during ongoing and sensory-evoked activities. *Nature Neurosci.* **11,** 535–537 (2008).
29. Dunn, F. A., Lankheet, M. J. & Rieke, F. Light adaptation in cone vision involves switching between receptor and post-receptor sites. *Nature* **449,** 603–606 (2007).
30. van Hateren, J. H. & Snippe, H. P. Information theoretical evaluation of parametric models of gain control in blowfly photoreceptor cells. *Vision Res.* **41,** 1851–1865 (2001).
31. Sharp, A. A., O'Neil, M. B., Abbott, L. F. & Marder, E. Dynamic clamp: computer-generated conductances in real neurons. *J. Neurophysiol.* **69,** 992–995 (1993).

Supplementary Information is linked to the online version of the paper at www.nature.com/nature.

Acknowledgements We thank D. Dacey, O. Packer, J. Crook, B. Peterson and T. Haun for providing primate tissue; P. Newman and E. Martinson for technical assistance; T. Azevedo, E. J. Chichilnisky, F. Dunn, G. Murphy, S. Kuo, E. Shea-Brown, M. Shadlen and W. Spain for comments on the manuscript and discussions. Support was provided by HHMI and NIH (EY-11850).

Author Contributions J.C. and F.R. designed and carried out the experiments, J.C. analysed the data and J.C. and F.R. wrote the paper.

Author Information Reprints and permissions information is available at www.nature.com/reprints. The authors declare no competing financial interests. Readers are welcome to comment on the online version of this article at www.nature.com/nature. Correspondence and requests for materials should be addressed to F.R. (rieke@u.washington.edu).

METHODS

Electrical recordings were made from midget ganglion cells in primate and ON–OFF DSGCs in mouse retinas as previously described[23,29]. Midget ganglion cells were identified by their relatively sustained response to light steps and characteristic morphology[17,29,32]. ON–OFF DSGCs were identified by a combination of at least two of the following criteria: an on–off light response to a brief light step, a bistratified morphology and a directionally selective spike response.

Light stimuli were delivered from light-emitting diodes or an organic light-emitting diode monitor (eMagin). Mean light levels for all experiments were near 5000 absorbed photons per cone per second. Full-field stimuli consisted of 10 s of constant light followed by 10 s of 50%-contrast modulated light (low-pass-filtered at 60 Hz) repeated for 5–20 trials. Moving bars were 180 μm wide, 720 μm long, moved at 864 μm s^{-1} along the long axis and had a contrast of between 100 and 150%.

For all recordings a flat-mounted piece of retina was superfused with warmed (31–34 °C) and oxygenated (5% CO_2, 95% O_2) Ames solution. Midget cell dynamic-clamp experiments were performed with receptors mediating excitatory and inhibitory synaptic input blocked (10 μM NBQX, 1 μM stychnine, 10 μM gabazine). Pipettes for voltage-clamp recordings were filled with a Cs-based internal solution (105 mM $CsCH_3SO_3$, 10 mM TEA-Cl, 20 mM HEPES, 10 mM EGTA, 5 mM Mg-ATP, 0.5 mM Tris-GTP and 2 mM QX-314, pH ~7.3, ~280 mosM). Pipettes for dynamic-clamp experiments were filled with a K-based internal solution (110 mM K aspartate, 1 mM MgCl, 10 mM HEPES, 5 mM NMDG, 0.5 mM $CaCl_2$, 10 mM phosphocreatine, 4 mM Mg-ATP and 0.5 mM Tris-GTP, pH ~7.2, ~280 mosM). Liquid junction potentials were ~10 mV and were not compensated throughout the text. Low access resistance was critical, and only cells with access resistance below 20 MΩ were included for analysis. Access resistance was partially compensated for (75% for experiments using an Axopatch 200B amplifier; 50% compensation and prediction for experiments using a Multiclamp 700B amplifier). Conductances were derived from excitatory and inhibitory synaptic currents by dividing the currents by assumed driving forces corresponding to voltages of −62 and +62 mV, respectively.

Both ganglion cell types showed evidence for NMDA-receptor-mediated conductances (J-shaped I–V plots that became linear in the presence of 10 μM APV). The presence of an NMDA conductance could cause noise correlations to be substantially underestimated if the voltage is substantially below the excitatory reversal potential. However, we observed only a weak impact of this conductance when noise correlations were compared before and after application of APV. Results from two cells recorded only in the presence of APV were included in the full data set.

The 10-ms cycle period during the simultaneous conductance recordings allows us to resolve input at 50 Hz and below. The fraction of the measured current variance at this cycle time was determined by calculating the fraction of the variance of the non-simultaneous (constant-voltage) conductances that can be accounted for by the variance of the simultaneous conductances.

Signal-to-noise ratios of spike outputs were calculated by forming spike trains of zeroes and ones from each trial, with 1-ms resolution. The mean and trial residuals of these spike trains were calculated and the power spectra of these functions were assessed and corrected for sample number bias[30]. Power spectra were integrated between 1 and 20Hz and the result for the mean responses was divided by that for the residuals (Supplementary Fig. 6).

Spike number in ON–OFF DSGCs in response to the moving bar was summed over the entire duration of the bar's movement. The direction selectivity index[10] was calculated as DSI = $|\sum \mathbf{v}_i / \sum \boldsymbol{r}_i|$, where $\mathbf{v}_i$ are vectors of lengths $\boldsymbol{r}_i$, equal to the normalized firing rate, and point in the direction of the moving bar that produced the presented conductances.

Current injected into a cell (I) during dynamic-clamp experiments[31] was calculated as

$$I(t) = G_{\mathrm{exc}}(t)(V(t-\Delta t) - E_{\mathrm{exc}}) + G_{\mathrm{inh}}(t)(V(t-\Delta t) - E_{\mathrm{inh}})$$

where G_{exc} and G_{inh} are a pair of conductances recorded during light stimulation, V is the cell's membrane potential, and E_{exc} and E_{inh} are reversal potentials set respectively at 0 mV and −80 mV. Changing the inhibitory reversal potential, E_{inh}, to −50 mV did not substantially affect the results.

Correlations were calculated using the 'xcov' function in MATLAB, release 2009a (MathWorks) and normalized using the 'coef' option. Briefly, this function calculates the cross-correlation after subtracting the means from each trial and normalizes by the geometric mean of the autocorrelation (see Supplementary Information, equation (2.1)).

32. Polyak, S. & Willmer, E. N. Retinal structure and colour vision. *Doc. Ophthalmol.* **3,** 24–56 (1949).